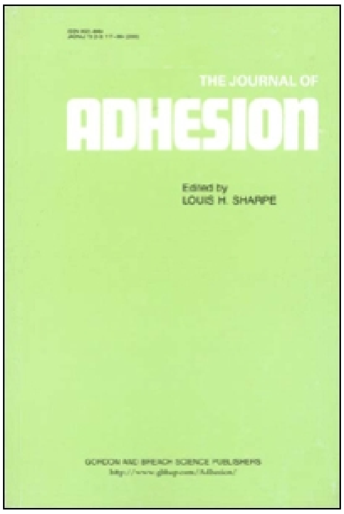

The Journal of Adhesion
Publication details, including instructions for authors and subscription information:
http://www.informaworld.com/smpp/title~content=t713453635

A Closed-form Solution for the Torque Transmission Capability of the Adhesively Bonded Tubular Double Lap Joint

Su Jeong Lee[a]; Dai Gil Lee[a]
[a] Department of Precision Engineering and Mechatronics, Korea Advanced Institute of Science and Technology, Taejon, Korea

To cite this Article Lee, Su Jeong and Lee, Dai Gil(1994) 'A Closed-form Solution for the Torque Transmission Capability of the Adhesively Bonded Tubular Double Lap Joint', The Journal of Adhesion, 44: 4, 271 — 284
To link to this Article: DOI: 10.1080/00218469408027083
URL: http://dx.doi.org/10.1080/00218469408027083

J. Adhesion, 1994, Vol. 44, pp. 271–284
Reprints available directly from the publisher
Photocopying permitted by license only

A Closed-form Solution for the Torque Transmission Capability of the Adhesively Bonded Tubular Double Lap Joint

SU JEONG LEE and DAI GIL LEE

Department of Precision Engineering and Mechatronics, Korea Advanced Institute of Science and Technology, Kusong-dong, Yusong-Ku, Taejon, Korea 305-701

(Received October 25, 1993; in final form May 10, 1994)

The adhesively bonded tubular double lap joint has better torque transmission capability and reliability in bonding than the single lap joint.

In this paper, an analytic solution for the torque transmission capability and stress distribution of the adhesively bonded tubular double lap joint was derived assuming linear properties of the adhesive.

From the analytic solution, it was found that the torque transmission capability of the double lap joint was more than 40% larger than that of the single lap joint.

KEY WORDS adhesive joint; double lap joint; analytical solution; stress distribution; comparison with single lap joint; effect of adhesive and adherend thickness; theory.

INTRODUCTION

Epoxy adhesives which are used to join mechanical elements are usually rubber toughened, which endows such adhesives with nonlinear properties. The mechanical elements joined by adhesives with nonlinear properties behave nonlinearly and the exact solutions of their behaviors can not be easily obtained. The exact solutions of the adhesively bonded joint were only possible with several assumptions such as linear elastic behaviors of the adhesive and the adherend.

Many researches on adhesive joints were performed after Adams[1] obtained the elastic solution of the adhesively bonded tubular single lap joint. The time-dependent visco-elastic behavior of the adhesive was included in the investigation of the adhesively bonded joint by Alwar and Nagaraja.[2] The torque transmission capabilities of partially-tapered tubular scarf joints were investigated by Adams and Peppiatt.[1]

The behaviors of adhesively bonded joints whose adherends were made of composite materials were investigated by several researchers[3,4,5] and several types of adhesively bonded joints such as the double lap, the single lap, the scarf, and the stepped-lap joint were analyzed by Hart-Smith.[6] The effect of the adhesive thickness and adherend roughness on the torsional fatigue strength of the adhesively bonded tubular single lap joint was investigated by Lee *et al.*,[7] and the failure model for the adhesively bonded tubular single lap joint was developed by Lee and Lee.[8]

Even though there are many such investigations on adhesively bonded joints, the simple linear elastic solution developed by Adams[1] is used in the first stage of design of the adhesively bonded joint because the dynamic or fatigue strength of the adhesively bonded tubular single lap joint can not be easily predicted using the accurately calculated static stress.

Even though the linear analytic solution for the adhesively bonded joint has the defect that it underestimates the torque transmission capabilities, it is widely used because it is simple and reveals the design parameters.

Therefore, in this paper, the shear stess distribution of the adhesively bonded tubular double lap joint under a torque was derived assuming linear properties of the adhesive. Also, the torque transmission capability of the adhesively bonded tubular double lap joint was calculated and compared with that of the single lap joint.

STRESS AND TORQUE CALCULATIONS

Figure 1 shows the configuration of the adhesively bonded tubular double lap joint and Figure 2 shows the deformation shapes and torque transmission variation of the sections at axial distances z and $z+\Delta z$.

In order to derive the analytic solution, two assumptions-that the adherends were under only the shear stress $\tau_{\theta z}$, and that the adhesive was under only the shear stress $\tau_{r\theta}$- were made. The shear moduli of the adherend and the adhesive were represented by $G_{\theta z}$ and $G_{r\theta}$, respectively. The analytic solution derived with the previous assumptions can be applied to the joint whose adherends are made of composite materials which have orthotropic properties.

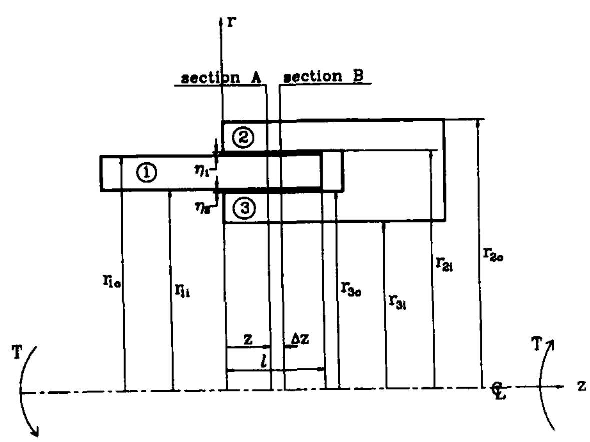

FIGURE 1 Configuration of the adhesively bonded tubular double lap joint (① represents the male adherend, ② and ③ represent the outer and inner layers of the female adherend, respectively).

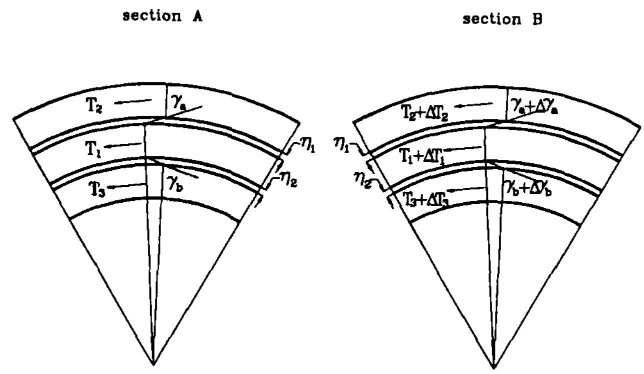

FIGURE 2 Torques and shear strains on the cross-sections at $z = z$ and $z + \Delta z$ of the adhesively bonded tubular double lap joint of Fig. 1.

By the geometric compatibility of the joint in Figure 2, the following equations can be derived.

$$(\gamma_a + \Delta\gamma_a)\eta_1 - \gamma_a\eta_1 = \gamma_{2i}\Delta z - \gamma_{1o}\Delta z \tag{1}$$

$$(\gamma_b + \Delta\gamma_b)\eta_2 - \gamma_b\eta_2 = -\gamma_{1i}\Delta z + \gamma_{3o}\Delta z \tag{2}$$

where,

$$\eta_1 = r_{2i} - r_{1o}$$

$$\eta_2 = r_{1i} - r_{3o}$$

r_{1i} and r_{2i} are the inner radii of adherends ① and ②, respectively, r_{1o} and r_{3o} are the outer radii of adherends ① and ③, respectively, γ_a is the shear strain of the outer adhesive, γ_b is the shear strain of the inner adhesive, γ_{1i} and γ_{2i} are shear strains at the inner surfaces of the adherends ① and ②, respectively, and γ_{1o} and γ_{3o} are the shear strains at the outer surfaces of the adherends ① and ③, respectively.

Equations (1) and (2) can be simplified by taking the limit $\Delta z \to 0$, as follows.

$$\eta_1 \frac{d\gamma_a}{dz} = \gamma_{2i} - \gamma_{1o} \tag{3}$$

$$\eta_2 \frac{d\gamma_b}{dz} = -\gamma_{1i} + \gamma_{3o} \tag{4}$$

Assuming the adhesive thickness is very small, the equilibrium conditions of Figure 2 are expressed as follows.

$$T_2 + \Delta T_2 - T_2 = \tau_a 2\pi a^2 \Delta z \tag{5}$$

$$T_3 + \Delta T_3 - T_3 = \tau_b 2\pi b^2 \Delta z \tag{6}$$

$$T_1 + \Delta T_1 - T_1 = -\tau_a 2\pi a^2 \Delta z - \tau_b 2\pi b^2 \Delta z \tag{7}$$

where,

$$a = \frac{r_{1o} + r_{2i}}{2}$$

$$b = \frac{r_{1i} + r_{3o}}{2}$$

and τ_a and τ_b are the shear stresses in the outer and inner adhesive, respectively, T_1, T_2 and T_3 are the torques in the adherends ①, ② and ③, respectively. Taking the limit $\Delta z \to 0$, Equations (5), (6) and (7) become as follows

$$\frac{dT_2}{dz} = 2\pi a^2 \tau_a \tag{8}$$

$$\frac{dT_3}{dz} = 2\pi b^2 \tau_b \tag{9}$$

$$\frac{dT_1}{dz} = -2\pi a^2 \tau_a - 2\pi b^2 \tau_b \tag{10}$$

Torques T_1, T_2 and T_3 should satisfy the following equation.

$$T = T_1 + T_2 + T_3 = \frac{\tau_{1o} J_1}{r_{1o}} + \frac{\tau_{2i} J_2}{r_{2i}} + \frac{\tau_{3o} J_3}{r_{3o}} \tag{11}$$

where J_1, J_2 and J_3 are the polar moments of inertia of adherends ①, ② and ③, respectively, r_{1o} is the outer radius of the adherend ①, r_{2i} is the inner radius of the adherend ②, r_{3o} is the outer radius of the adherend ③, and τ_{1o}, τ_{2i} and τ_{3o} are the shear stresses of adherends at $r = r_{1o}$, $r = r_{2i}$ and $r = r_{3o}$, respectively.

Substituting Equation (3) and $\tau_a = G_a \gamma_a$ into Equation (8) yields the following relationship.

$$\begin{aligned} \eta_1 \frac{d^2 T_2}{dz^2} &= 2\pi a^2 \eta_1 \frac{d\tau_a}{dz} \\ &= 2\pi a^2 \eta_1 G_a \frac{d\gamma_a}{dz} \\ &= 2\pi a^2 G_a (\gamma_{2i} - \gamma_{1o}) \\ &= 2\pi a^2 G_a \left(\frac{\tau_{2i}}{G_2} - \frac{\tau_{1o}}{G_1} \right) \end{aligned} \tag{12}$$

Substituting the relationship $d^2T_2/dz^2 = d^2/dz^2 (\tau_{2i} J_2 / r_{2i})$ into Equation (12) yields the following equation.

$$\frac{d^2 \tau_{2i}}{dz^2} = 2\pi a^2 G_a \frac{1}{\eta_1} \frac{r_{2i}}{J_2} \left(\frac{\tau_{2i}}{G_2} - \frac{\tau_{1o}}{G_1} \right) \tag{13}$$

When the outer and the inner adhesives are made of the same material ($G_a = G_b$), substituting Equation (4) and $\tau_b = G_a \gamma_b$ into Equation (8) yields the following relationship.

$$\eta_2 \frac{d^2 T_3}{dz^2} = 2\pi b^2 \eta_2 \frac{d\tau_b}{dz}$$

$$= 2\pi b^2 \eta_2 G_a \frac{d\gamma_b}{dz} \tag{14}$$

$$= -2\pi b^2 G_a(\gamma_{1i} - \gamma_{3o})$$

$$= -2\pi b^2 G_a\left(\frac{\tau_{1i}}{G_1} - \frac{\tau_{3o}}{G_3}\right)$$

Substituting the relationship $d^2T_3/dz^2 = d^2/dz^2(\tau_{3o}J_3/r_{3o})$ into Equation (14) yields the following equation.

$$\frac{d^2\tau_{3o}}{dz^2} = -2\pi b^2 G_a \frac{1}{\eta_2}\frac{r_{3o}}{J_3}\left(\frac{\tau_{1i}}{G_1} - \frac{\tau_{3o}}{G_3}\right) \tag{15}$$

Since the relationship $T = T_1 + T_2 + T_3$ holds throughout the joint length, and $T_1 = 0$ at $z = l$, the relationship of torques at $z = l$ becomes:

$$T = T_{2l} + T_{3l} = \frac{\tau_{2il}J_2}{r_{2i}} + \frac{\tau_{3ol}J_3}{r_{3o}} \tag{16}$$

From Equation (11) and (16), the shear stress τ_{1o} at $r = r_{1o}$ becomes:

$$\tau_{1o} = \frac{r_{1o}}{J_1}\left(T - \frac{\tau_{2i}J_2}{r_{2i}} - \frac{\tau_{3o}J_3}{r_{3o}}\right) \tag{17}$$

Substituting Equation (17) into (13) yields the following equation.

$$\frac{d^2\tau_{2i}}{dz^2} = 2\pi a^2 G_a \frac{1}{\eta_1}\frac{r_{2i}}{J_2}\left[\frac{\tau_{2i}}{G_2} - \frac{r_{1o}}{G_1 J_1}\left(T - \frac{\tau_{2i}J_2}{r_{2i}} - \frac{\tau_{3o}J_3}{r_{3o}}\right)\right]$$

$$= 2\pi a^2 G_a \frac{1}{\eta_1}\left(\frac{r_{2i}}{J_2 G_2} + \frac{r_{1o}}{J_1 G_1}\right)\tau_{2i} - 2\pi a^2 G_a \frac{1}{\eta_1}\frac{r_{2i}}{J_2}\frac{r_{1o}}{G_1 J_1}T \tag{18}$$

$$+ 2\pi a^2 G_a \frac{1}{\eta_1}\frac{r_{2i}}{J_2}\frac{r_{1o}}{G_1 J_1}\frac{J_3}{r_{3o}}\tau_{3o}$$

when $r = r_{1i}$, the shear stress τ_{1i} can be derived by the same method used in deriving Equation (17) as follows:

$$\tau_{1i} = \frac{r_{1i}}{J_1}\left(T - \frac{\tau_{2i}J_2}{r_{2i}} - \frac{\tau_{3o}J_3}{r_{3o}}\right) \tag{19}$$

Substituting Equation (19) into Equation (15) yields the following equation.

$$\frac{d^2\tau_{3o}}{dz^2} = -2\pi b^2 G_a \frac{1}{\eta_2}\frac{r_{3o}}{J_3}\left[\frac{r_{1i}}{G_1 J_1}\left(T - \frac{\tau_{2i}J_2}{r_{2i}} - \frac{\tau_{3o}J_3}{r_{3o}}\right) - \frac{\tau_{3o}}{G_3}\right]$$

$$= 2\pi b^2 G_a \frac{1}{\eta_2}\left(\frac{r_{1i}}{J_1 G_1} + \frac{r_{3o}}{J_3 G_3}\right)\tau_{3o} - 2\pi b^2 G_a \frac{1}{\eta_2}\frac{r_{1i}}{G_1 J_1}\frac{r_{3o}}{J_3}T \tag{20}$$

$$+ 2\pi b^2 G_a \frac{1}{\eta_2}\frac{r_{3o}}{J_3}\frac{r_{1i}}{G_1 J_1}\frac{J_2\tau_{2i}}{r_{2i}}$$

Equations (18) and (20) can be simplified as follows:

$$\frac{d^2\tau_{2i}}{dz^2} = \alpha_1\tau_{2i} + \alpha_2 + \alpha_3\tau_{3o} \tag{21}$$

$$\frac{d^2\tau_{3o}}{dz^2} = \alpha_4\tau_{3o} + \alpha_5 + \alpha_6\tau_{2i} \tag{22}$$

where,

$$\alpha_1 = 2\pi a^2 G_a \frac{1}{\eta_1}\left(\frac{r_{2i}}{J_2G_2} + \frac{r_{1o}}{J_1G_1}\right)$$

$$\alpha_2 = -2\pi a^2 G_a \frac{1}{\eta_1}\frac{r_{2i}}{J_2}\frac{r_{1o}}{G_1J_1}T$$

$$\alpha_3 = 2\pi a^2 G_a \frac{1}{\eta_1}\frac{r_{2i}}{J_2}\frac{r_{1o}}{G_1J_1}\frac{J_3}{r_{3o}}$$

$$\alpha_4 = 2\pi b^2 G_a \frac{1}{\eta_2}\left(\frac{r_{1i}}{J_1G_1} + \frac{r_{3o}}{J_3G_3}\right)$$

$$\alpha_5 = -2\pi b^2 G_a \frac{1}{\eta_2}\frac{r_{1i}}{G_1J_1}\frac{r_{3o}}{J_3}T$$

$$\alpha_6 = 2\pi b^2 G_a \frac{1}{\eta_2}\frac{r_{3o}}{J_3}\frac{r_{1i}}{G_1J_1}\frac{J_2}{r_{2i}}$$

From Equation (21), τ_{3o} can be expressed as

$$\tau_{3o} = \frac{1}{\alpha_3}\left(\frac{d^2\tau_{2i}}{dz^2} - \alpha_1\tau_{2i} - \alpha_2\right) \tag{23}$$

Substituting Equation (23) into Equation (22) yields the following fourth-order ordinary differential equation.

$$\frac{d^4\tau_{2i}}{dz^4} - (\alpha_1 + \alpha_4)\frac{d^2\tau_{2i}}{dz^2} + (\alpha_1\alpha_4 - \alpha_3\alpha_6)\tau_{2i} + (\alpha_2\alpha_4 - \alpha_3\alpha_5) = 0 \tag{24}$$

Equation (24) can be simplified using three parameters β_1, β_2 and β_3 as follows:

$$\frac{d^4\tau_{2i}}{dz^4} + \beta_1\frac{d^2\tau_{2i}}{dz^2} + \beta_2\tau_{2i} + \beta_3 = 0 \tag{25}$$

where,

$$\beta_1 = -(\alpha_1 + \alpha_4)$$

$$\beta_2 = \alpha_1\alpha_4 - \alpha_3\alpha_6$$

$$\beta_3 = \alpha_2\alpha_4 - \alpha_3\alpha_5$$

The solution of Equation (25) is expressed as

$$\tau_{2i} = A \cdot \sinh(\lambda_1 z) + B \cdot \sinh(\lambda_2 z) + C \cdot \cosh(\lambda_1 z) + D \cdot \cosh(\lambda_2 z) - \frac{\beta_3}{\beta_2} \tag{26}$$

where

$$\lambda_1, \lambda_2 = \sqrt{\frac{-\beta_1 \pm \sqrt{\beta_1^2 - 4\beta_2}}{2}}$$

and, A, B, C and D are constants which can be determined by boundary conditions. The boundary conditions of Equation (26) are

$$\text{At } z = 0, \quad \tau_{2i} = 0 \quad \text{and} \quad \tau_{3o} = 0 \tag{27}$$

Therefore, Equation (21) at $z = 0$ becomes

$$\frac{d^2\tau_{2i}}{dz^2} = \alpha_1\tau_{2i} + \alpha_2 + \alpha_3\tau_{3o} = \alpha_2 \tag{28}$$

Since at

$$z = l, \quad \tau_{2i} = \frac{r_{2i}T}{J_2 + J_3} \quad \text{and} \quad \tau_{3o} = \frac{r_{3o}T}{J_2 + J_3} \tag{29}$$

Equation (21) at $z = l$ becomes

$$\frac{d^2\tau_{2i}}{dz^2} = \alpha_1\tau_{2i} + \alpha_2 + \alpha_3\tau_{3o}$$

$$= \alpha_1\frac{r_{2i}T}{J_2 + J_3} + \alpha_2 + \alpha_3\frac{r_{3o}T}{J_2 + J_3} \tag{30}$$

Substituting Equations (27) and (28) into Equation (26) yields the following equations.

$$\tau_{2i} = C + D - \frac{\beta_3}{\beta_2} = 0 \tag{31}$$

$$\frac{d^2\tau_{2i}}{dz^2} = \lambda_1^2 C + \lambda_2^2 D = \alpha_2 \tag{32}$$

Substituting Equations (29) and (30) into Equation (26) yields the following equations.

$$\tau_{2i} = A \cdot \sinh(\lambda_1 l) + B \cdot \sinh(\lambda_2 l) + C \cdot \cosh(\lambda_1 l) + D \cdot \cosh(\lambda_2 l) - \frac{\beta_3}{\beta_2} \tag{33}$$

$$= \frac{r_{2i}T}{J_2 + J_3}$$

$$\frac{d^2\tau_{2i}}{dz^2} = A\lambda_1^2 \cdot \sinh(\lambda_1 l) + B\lambda_2^2 \cdot \sinh(\lambda_2 l) + C\lambda_1^2 \cdot \cosh(\lambda_3 l) + D\lambda_2^2 \cdot \cosh(\lambda_4 l)$$

$$= \alpha_2 + \frac{\alpha_1 r_{2i} + \alpha_3 r_{3o}}{J_2 + J_3} T \tag{34}$$

The integrating constants can be calculated from Equations (31), (32), (33) and (34) as follows:

$$A=\frac{1}{(\lambda_2^2-\lambda_1^2)\ \sinh(\lambda_1 l)}\left[\lambda_2^2\frac{\beta_3}{\beta_2}-\alpha_2-\frac{\alpha_1 r_{2i}+\alpha_3 r_{3o}-\lambda_2^2 r_{2i}}{J_2+J_3}T\right.$$

$$\left.-C(\lambda_2^2-\lambda_1^2)\cosh(\lambda_1 l)\right] \quad (35\text{-a})$$

$$B=\frac{1}{(\lambda_1^2-\lambda_2^2)\ \sinh(\lambda_2 l)}\left[\lambda_1^2\frac{\beta_3}{\beta_2}-\alpha_2-\frac{\alpha_1 r_{2i}+\alpha_3 r_{3o}-\lambda_1^2 r_{2i}}{J_2+J_3}T\right.$$

$$\left.-D(\lambda_1^2-\lambda_2^2)\cosh(\lambda_2 l)\right] \quad (35\text{-b})$$

$$C=\frac{\lambda_2^2\frac{\beta_3}{\beta_2}-\alpha_2}{\lambda_2^2-\lambda_1^2} \quad (35\text{-c})$$

$$D=\frac{\alpha_2-\lambda_1^2\frac{\beta_3}{\beta_2}}{\lambda_2^2-\lambda_1^2} \quad (35\text{-d})$$

Substituting Equation (26) and the relationship $T_2=\tau_{2i}J_2/r_{2i}$ into Equation (8), the shear stress τ_a at the outer adhesive can be calculated from the following

$$\tau_a=\frac{J_2}{2\pi a^2 r_{2i}}[A\lambda_1\cosh(\lambda_1 z)+B\lambda_2\cosh(\lambda_2 z)+C\lambda_1\sinh(\lambda_1 z)+D\lambda_2\sinh(\lambda_2 z)] \quad (36)$$

Substituting Equation (26) into Equation (23), the shear stress τ_{3o} of the adherend ③ at $r=r_{3o}$ can be calculated as follows:

$$\tau_{3o}=\frac{1}{\alpha_3}\{A(\lambda_1^2-\alpha_1)\sinh(\lambda_1 z)+B(\lambda_2^2-\alpha_2)\sinh(\lambda_2 z)$$

$$+C(\lambda_1^2-\alpha_3)\cosh(\lambda_1 z)+D(\lambda_2^2-\alpha_4)\cosh(\lambda_2 z)-\alpha_2\} \quad (37)$$

Substituting Equation (36) and the relationship $T_3=\tau_{3o}J_3/r_{3o}$ into Equation (9) yields the following shear stress distribution in the inner adhesive.

$$\tau_b=\frac{J_3}{2\pi b^2 r_{3o}\alpha_3}\{A(\lambda_1^2+\alpha_1)\lambda_1\cosh(\lambda_1 z)+B(\lambda_2^2+\alpha_2)\lambda_2\cosh(\lambda_2 z)$$

$$+C(\lambda_1^2+\alpha_3)\lambda_1\sinh(\lambda_1 z)+D(\lambda_2^2+\alpha_4)\lambda_2\sinh(\lambda_2 z)\} \quad (38)$$

The shear stress in adherend ① can be calculated by substituting Equations (34) and (38) into Equation (11) as follows:

$$\begin{aligned}
\tau_{1o} &= \frac{r_{1o}}{J_1}\left(T - \frac{\tau_{2i}J_2}{r_{2i}} - \frac{\tau_{3o}J_3}{r_{3o}}\right) \\
&= \frac{r_{1o}}{J_1}\left\{T - A\left(\frac{J_2}{r_{2i}} + \frac{J_3}{r_{3o}}\frac{\lambda_1^2 - \alpha_1}{\alpha_3}\right)\sinh(\lambda_1 z)\right. \\
&\quad - B\left(\frac{J_2}{r_{2i}} + \frac{J_3}{r_{3o}}\frac{\lambda_2^2 - \alpha_1}{\alpha_3}\right)\sinh(\lambda_2 z) \\
&\quad - C\left(\frac{J_2}{r_{2i}} + \frac{J_3}{r_{3o}}\frac{\lambda_1^2 - \alpha_1}{\alpha_3}\right)\cosh(\lambda_1 z) \\
&\quad \left. - D\left(\frac{J_2}{r_{2i}} + \frac{J_3}{r_{3o}}\frac{\lambda_2^2 - \alpha_1}{\alpha_3}\right)\cosh(\lambda_2 z) + \frac{J_2}{r_{2i}}\frac{\beta_3}{\beta_2} + \frac{J_3}{r_{3o}}\frac{\alpha_2}{\alpha_3}\right\}
\end{aligned} \tag{39}$$

up to now, shear stresses in adherends ①, ② and ③ as well as shear stresses in the inner and outer adhesives were all found.

NUMERICAL EXAMPLES

The shear stress distributions in the adhesives of the adhesively bonded tubular single lap and double lap joints under torsional loadings were calculated, in order to compare the torque transmission capabilities of the joints. Dimensions of the joints used in the numerical example are shown in Table I and the symbols in Table I are depicted in Figure 1. Dimensions of the single lap joint were selected to be the same as those of the

TABLE I
Simulation conditions of the torque transmission capabilities of adhesively bonded tubular single and double lap joints

	Single lap joint	Double lap joint	Note
r_{1o}(mm)	30.0	30.0	t_{ad}① = 3.0 mm
r_{1i}(mm)	27.0	27.0	
r_{2o}(mm)	Not applicable	33.1/34.0	t_{ad}② = 3.0 mm
r_{2i}(mm)	Not applicable	30.1/34.0	
r_{3o}(mm)	26.9/26.0	26.9/26.0	t_{ad}③ = 3.0 mm
r_{3i}(mm)	23.9/23.0	23.9/23.0	
η(mm)	0.1/1.0	0.1/1.0	two different adhesive thicknesses
l(mm)	40.0	40.0	
Shear modulus of the adherend (GPa)	76.9	76.9	Steel
Shear modulus of the adhesive (GPa)	0.461	0.461	IPCO 9923 Epoxy adhesive
Shear strength of the adhesive (MPa)	30.0	30.0	

t_{ad} = thickness of the adherend

double lap joint except that the outer layer ② of the female adherend was removed from the double lap joint of Figure 1. Figure 3 shows the configuration of the single lap joint. The analytical solution of the single lap joint by Adams[1] is summarized in the Appendix of this paper.

Although there are many parameters for the design of adhesively bonded tubular double lap joints, such as r_{1o}, r_{1i}, r_{2o}, r_{2i}, r_{3o}, r_{3i}, G_a, G_1, G_2, G_3 and l, in this paper the stress distributions of the single lap and double lap joints were calculated under the same torque, fixing these parameters with the typical design values.

Figure 4 shows the shear stress distributions in the adhesives in joints when the applied torque was 1,000 N · m. From Figure 4, it was found that the magnitude of the shear stress of the double lap joint was less than that of the single lap joint, and both the single lap and double lap joints with 1.0 mm adhesive thickness (Fig. 4b) had lower stress concentration than joints with 0.1 mm adhesive thickness (Fig. 4a).

Table II shows the torque transmission capabilities of the joints when the adhesive shear strength was 30 MPa. In Table II, the torque transmission capabilities of double lap joints with 0.1 and 1.0 mm adhesive thicknesses were improved 46 and 61%, respectively, compared with those of the single lap joints.

An efficiently designed adhesively bonded tubular double lap joint should have a low level of the shear stress distribution, and the magnitudes of the shear stresses in the inner and outer adhesive layers should be same, which can be accomplished by adjusting the thicknesses of the inner and outer layers of the female adherends. To this end, the thicknesses of the inner and outer layers of the female adherend of the double lap joint were varied from 0.5 to 4.0 mm with other dimensions and material properties fixed as shown in Table III. The thickness of the male adherend was fixed at 3.0 mm.

Figure 5 shows the distributions of the torque transmission capabilties of the double lap joints with respect to the thicknesses of the inner and outer layers of the female adherends when the adhesive shear strength was 30 MPa, and the thickness of the male adherend was 3.0 mm. Table IV shows the conditions for the maximum torque

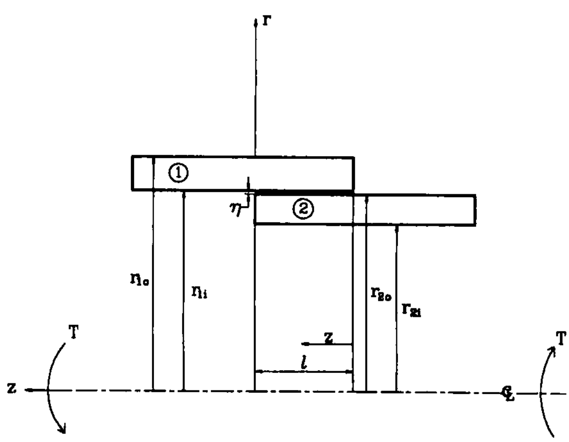

FIGURE 3 Configuration of the adhesively bonded tubular single lap joint (① represents the outer adherend, ② represents the inner adherend).

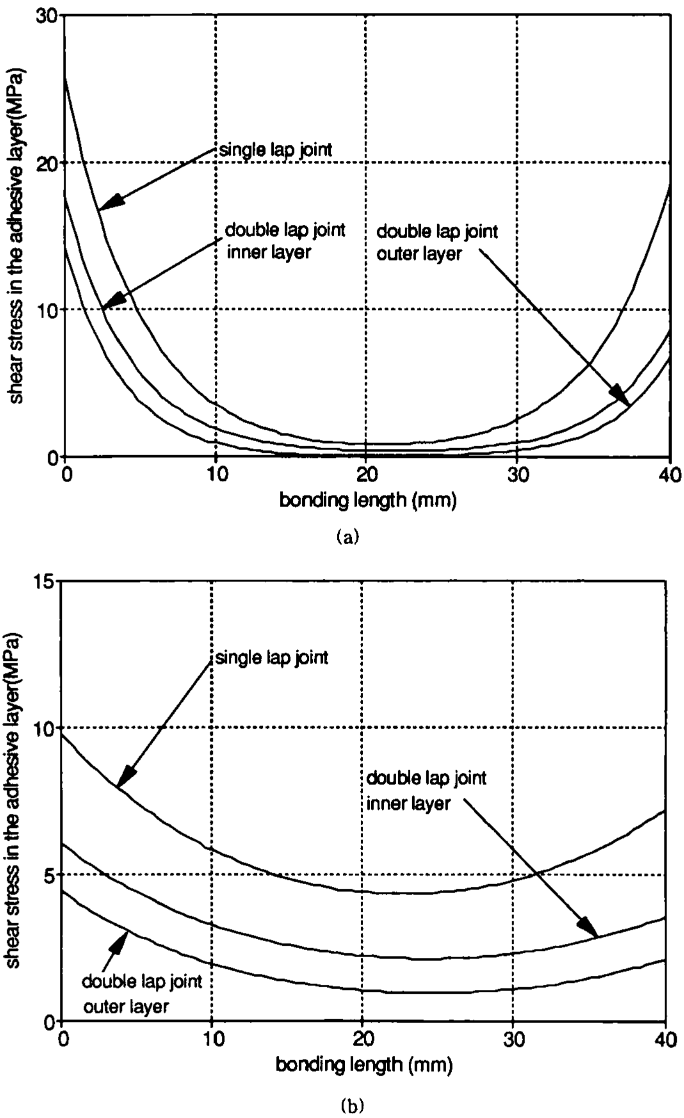

FIGURE 4 Shear stress distributions in the adhesive layers when the applied torque was 1000 N·m (a) 0.1 mm adhesive thickness (b) 1.0 mm adhesive thickness.

transmission capabilities. From Figure 4, it was found that there was only one condition for the maximum torque transmission capability for each adhesive thickness, in which the relationship $J_1 = J_2 + J_3$ is satisfied approximately. This relationship is similar to that of the adhesively bonded tubular double lap joint which has the maximum torque transmission capability when the magnitudes of polar moments of inertia of the two adherends are the same.

TABLE II
Calculated torque transmission capabilities of adhesively bonded tubular single and double lap joints when the adhesive shear strength was 30 MPa

	Single lap joint	Double lap joint	Note
0.1 mm adhesive thickness	1,162 Nm	1,702 Nm	46% improved
1.0 mm adhesive thickness	3,080 Nm	4,967 Nm	61% improved

TABLE III
Simulation conditions of the effect of the adherend thickness on the torque transmission capabilities

	t_{ad} of ②, ③ = 0.5 ~ 4.0 mm	
	0.1 mm adhesive thickness	1.0 mm adhesive thickness
r_{1o}(mm)	30.0	30.0
r_{1i}(mm)	27.0	27.0
r_{2o}(mm)	$30.1 + t_{ad}$②	$31.0 + t_{ad}$②
r_{2i}(mm)	30.1	31.0
r_{3o}(mm)	26.9	26.0
r_{3i}(mm)	$26.9 - t_{ad}$③	$26.0 - t_{ad}$③
η(mm)	0.1	
l(mm)	40.0	
Shear modulus of the adherend (Gpa)	76.9	
Shear modulus of the adhesive (GPa)	0.461	
Shear strength of the adhesive (MPa)	30.0	

t_{ad} = thickness of the adherend

TABLE IV
Parameter values of the adhesively bonded tubular double lap joint for the maximum torque transmission capability

	0.1 mm adhesive thickness	1.0 mm adhesive thickness
Thickness of the adherend ①(mm)	3.00	3.00
Thickness of the adherend ②(mm)	1.24	1.32
Thickness of the adherend ③(mm)	1.90	2.10
$J_1(10^{-7}\,m^4)$	4.376	4.376
$J_2(10^{-7}\,m^4)$	2.260	2.633
$J_3(10^{-7}\,m^4)$	2.089	2.530
Torque (N·m)	2,149	6,375

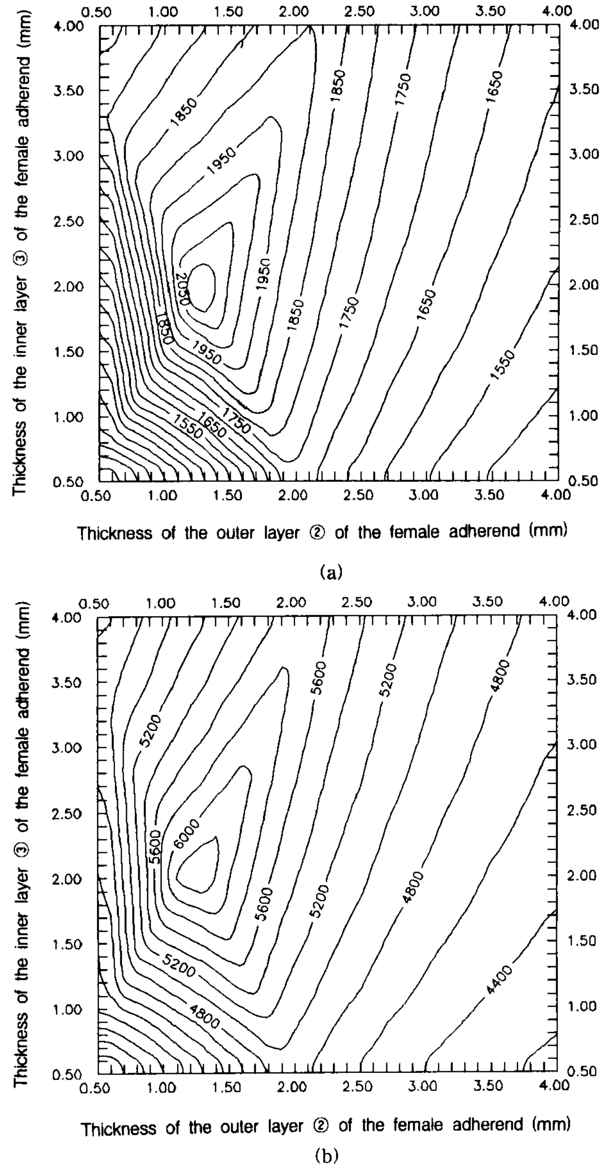

FIGURE 5 Distributions of the torque tranmission capabilities w.r.t. the thicknesses of the adherends ② and ③ when the adhesive shear strength was 30 MPa (a) 0.1 mm adhesive thickness (b) 1.0 mm adhesive thickness.

CONCLUSION

In this work, closed-form solutions for the stress distribution and torque transmission capability of the adhesively bonded tubular double lap joint were derived and compared with those of the single lap joint.

From the solution, it was found that the torque transmission capabilities of the double lap joint whose outer diameter was 68 mm were improved 46% and 61% compared with those of the single lap joint when adhesive thicknesses were 0.1 and 1.0 mm, respectively. Also, it was found that the adherend thickness for the maximum torque transmission capability was unique, such that the polar moments of inertia of the male and female adherends had the relationship $J_1 \approx J_2 + J_3$.

References

1. R. D. Adams, and N. A. Peppiatt, "Stress Analysis of Adhesive Bonded Tubular Lap Joints," *J. Adhesion* **9**, 1–18 (1977).
2. R. S. Alwar and Y. R. Nagaraja, "Viscoelastic Analysis of an Adhesive Tubular Joint," *J. Adhesion* **8**, 79–92 (1976).
3. O. T. Thomsen, and A. Kildegaard, "Analysis of Adhesive Bonded Generally Orthotropic Circular Shells," in *Developments in the Science and Technology of Composite Materials*, Proceedings of the Fourth European Conference of Composite Materials, pp. 723–729 (September 25–28, 1990, Stuttgart, Germany).
4. C. T. Chon, "Analysis of Tubular Lap Joint in Torsion," *J. Composite Mater.*, **16**, 268–284 (1982).
5. P. J. Hipol, "Analysis and Optimization of a Tubular Lap Joint Subjected to Torsion," *J. Composite Mater.* **18**, 298–311 (1984).
6. L. J. Hart-Smith, "Further Developments in the Design and Analysis of Adhesive Bonded Structural Joints in Joining of Composite Materials," **ASTM, STP 749**, 3–31 (1981).
7. D. G. Lee, K. S. Kim, and Y. T. Lim, "An Experimental Study of Fatigue Strength for Adhesively Bonded Tubular Single Lap Joints," *J. Adhesion* **35**, 39–53 (1991).
8. S. J. Lee, and D. G. Lee, "Development of a Failure Model for the Adhesively Bonded Tubular Single Lap Joint," *J. Adhesion* **40**, 1–14 (1992).

APPENDIX

The analytic solutions for the shear stress distribution in the adhesive of the adhesively bonded tubular single lap joint given by Adams[1] are summarized as follows.

$$\tau_a = \frac{T\alpha}{2\pi a^2}\left[\left\{\frac{1-\psi(1-\cosh(\alpha l))}{\sinh(\alpha l)}\right\}\cosh(\alpha z) - \psi\sinh(\alpha z)\right]$$

where

$$a = \frac{r_{1i} + r_{2o}}{2}$$

$$\delta = \frac{2\pi a^2 r_{2o} G_a}{G_2 J_2 \eta}$$

$$\psi = \frac{G_1 J_1 r_{2o}}{G_1 J_1 r_{2o} + G_2 J_2 r_{1i}}$$

$$\alpha = \sqrt{\frac{\delta}{\psi}}$$